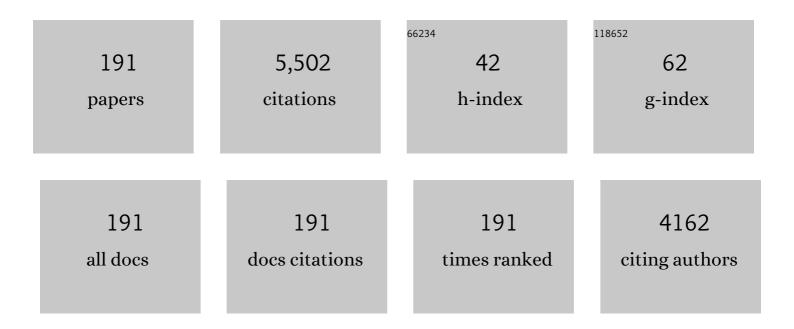
List of Publications by Year in descending order

Source: https://exaly.com/author-pdf/7588071/publications.pdf Version: 2024-02-01



IENS IENSEN

#	Article	IF	CITATIONS
1	On the film density using high power impulse magnetron sputtering. Surface and Coatings Technology, 2010, 205, 591-596.	2.2	317
2	B4C thin films for neutron detection. Journal of Applied Physics, 2012, 111, .	1.1	128
3	A review of metal-ion-flux-controlled growth of metastable TiAlN by HIPIMS/DCMS co-sputtering. Surface and Coatings Technology, 2014, 257, 15-25.	2.2	126
4	Role of Tin+ and Aln+ ion irradiation (n=1, 2) during Ti1-xAlxN alloy film growth in a hybrid HIPIMS/magnetron mode. Surface and Coatings Technology, 2012, 206, 4202-4211.	2.2	119
5	Toughness enhancement in hard ceramic thin films by alloy design. APL Materials, 2013, 1, .	2.2	109
6	Metal versus rare-gas ion irradiation during Ti1â^' <i>x</i> Al <i>x</i> N film growth by hybrid high power pulsed magnetron/dc magnetron co-sputtering using synchronized pulsed substrate bias. Journal of Vacuum Science and Technology A: Vacuum, Surfaces and Films, 2012, 30, .	0.9	98
7	Microstructure and dielectric properties of piezoelectric magnetron sputtered w-ScxAl1â^'xN thin films. Journal of Applied Physics, 2012, 111, .	1.1	93
8	Conetrap: A compact electrostatic ion trap. Nuclear Instruments & Methods in Physics Research B, 2001, 173, 523-527.	0.6	88
9	Characterization of swift heavy ion tracks in CaF2 by scanning force and transmission electron microscopy. Nuclear Instruments & Methods in Physics Research B, 2005, 240, 819-828.	0.6	88
10	Anomalously high thermoelectric power factor in epitaxial ScN thin films. Applied Physics Letters, 2011, 99, .	1.5	84
11	Layer formation by resputtering in Ti–Si–C hard coatings during large scale cathodic arc deposition. Surface and Coatings Technology, 2011, 205, 3923-3930.	2.2	83
12	Hysteresis and process stability in reactive high power impulse magnetron sputtering of metal oxides. Thin Solid Films, 2011, 519, 7779-7784.	0.8	82
13	Microstructure control of CrNx films during high power impulse magnetron sputtering. Surface and Coatings Technology, 2010, 205, 118-130.	2.2	77
14	Vacancy-induced toughening in hard single-crystal V 0.5 Mo 0.5 N x /MgO(0 0 1) thin films. Acta Materialia, 2014, 77, 394-400.	3.8	75
15	<pre>\$hbox{CrN}_{m x}\$ Films Prepared by DC Magnetron Sputtering and High-Power Pulsed Magnetron Sputtering: A Comparative Study. IEEE Transactions on Plasma Science, 2010, 38, 3046-3056.</pre>	0.6	72
16	Effect of peak power in reactive high power impulse magnetron sputtering of titanium dioxide. Surface and Coatings Technology, 2011, 205, 4828-4831.	2.2	70
17	Strain-free, single-phase metastable Ti0.38Al0.62N alloys with high hardness: metal-ion energy vs. momentum effects during film growth by hybrid high-power pulsed/dc magnetron cosputtering. Thin Solid Films, 2014, 556, 87-98.	0.8	69
18	Experimental and ab initio study of the mechanical properties of hydroxyapatite. Applied Physics Letters, 2007, 90, 193902.	1.5	68

#	Article	IF	CITATIONS
19	Selection of metal ion irradiation for controlling Ti1â^'xAlxN alloy growth via hybrid HIPIMS/magnetron co-sputtering. Vacuum, 2012, 86, 1036-1040.	1.6	66
20	Structural and mechanical properties of Cr–Al–O–N thin films grown by cathodic arc deposition. Acta Materialia, 2012, 60, 6494-6507.	3.8	65
21	Track separation due to dissociation of MeV C60 inside a solid. Nuclear Instruments & Methods in Physics Research B, 1997, 132, 93-108.	0.6	63
22	Wet-cleaning of MgO(001): Modification of surface chemistry and effects on thin film growth investigated by x-ray photoelectron spectroscopy and time-of-flight secondary ion mass spectroscopy. Journal of Vacuum Science and Technology A: Vacuum, Surfaces and Films, 2017, 35, .	0.9	63
23	Molecule and cluster bombardment: energy loss, trajectories, and collision cascades. Nuclear Instruments & Methods in Physics Research B, 1996, 112, 1-11.	0.6	60
24	Highly Charged Clusters of Fullerenes: Charge Mobility and Appearance Sizes. Physical Review Letters, 2003, 91, 215504.	2.9	60
25	Face-centered cubic (Al1â^'xCrx)2O3. Thin Solid Films, 2011, 519, 2426-2429.	0.8	60
26	Growth of High Quality Epitaxial Rhombohedral Boron Nitride. Crystal Growth and Design, 2012, 12, 3215-3220.	1.4	60
27	ZrB2 thin films grown by high power impulse magnetron sputtering from a compound target. Thin Solid Films, 2012, 526, 163-167.	0.8	58
28	Epitaxial growth and electrical transport properties of Cr <mml:math xmlns:mml="http://www.w3.org/1998/Math/MathML" display="inline"&gt;<mml:msub><mml:mrow /&gt;<mml:mn>2</mml:mn></mml:mrow </mml:msub>GeC thin films. Physical Review B, 2011, 84, .</mml:math 	1.1	56
29	Static over-the-barrier model for electron transfer between metallic spherical objects. Physical Review A, 2002, 66, .	1.0	55
30	Tracks induced in CaF2 by MeV cluster irradiation. Nuclear Instruments & Methods in Physics Research B, 1998, 141, 753-762.	0.6	54
31	Photodissociation of protonated amino acids and peptides in an ion storage ring. Determination of Arrhenius parameters in the high-temperature limit. Physical Chemistry Chemical Physics, 2004, 6, 2676-2681.	1.3	53
32	Stability of 10B4C thin films under neutron radiation. Radiation Physics and Chemistry, 2015, 113, 14-19.	1.4	53
33	Control of Tilâ^'xSixN nanostructure via tunable metal-ion momentum transfer during HIPIMS/DCMS co-deposition. Surface and Coatings Technology, 2015, 280, 174-184.	2.2	53
34	Power-law decay of collisionally excited amino acids and quenching by radiative cooling. European Physical Journal D, 2003, 25, 139-148.	0.6	52
35	Electronic-grade GaN(0001)/Al2O3(0001) grown by reactive DC-magnetron sputter epitaxy using a liquid Ga target. Applied Physics Letters, 2011, 98, .	1.5	52
36	ERD analysis and modification of TiO2 thin films with heavy ions. Nuclear Instruments & Methods in Physics Research B, 2010, 268, 1893-1898.	0.6	49

#	Article	IF	CITATIONS
37	Mitigating the geometrical limitations of conventional sputtering by controlling the ion-to-neutral ratio during high power pulsed magnetron sputtering. Thin Solid Films, 2011, 519, 6354-6361.	0.8	48
38	Lifetimes of C602â^' and C702â^' dianions in a storage ring. Journal of Chemical Physics, 2006, 124, 024310.	1.2	47
39	A comparison between tracks created by high energy mono-atomic and cluster ions in Y3Fe5O12. Nuclear Instruments & Methods in Physics Research B, 1998, 146, 412-419.	0.6	45
40	Phase stability and initial low-temperature oxidation mechanism of Ti2AlC thin films. Journal of the European Ceramic Society, 2013, 33, 375-382.	2.8	45
41	Effect of WN content on toughness enhancement in V1â^'xWxN/MgO(001) thin films. Journal of Vacuum Science and Technology A: Vacuum, Surfaces and Films, 2014, 32, .	0.9	45
42	Epitaxial CVD growth of sp <sup>2</sup> â€hybridized boron nitride using aluminum nitride as buffer layer. Physica Status Solidi - Rapid Research Letters, 2011, 5, 397-399.	1.2	44
43	Low-temperature growth of boron carbide coatings by direct current magnetron sputtering and high-power impulse magnetron sputtering. Journal of Materials Science, 2016, 51, 10418-10428.	1.7	44
44	CFx thin solid films deposited by high power impulse magnetron sputtering: Synthesis and characterization. Surface and Coatings Technology, 2011, 206, 646-653.	2.2	43
45	Ion track formation below 1MeV/u in thin films of amorphous SiO2. Nuclear Instruments & Methods in Physics Research B, 2006, 243, 119-126.	0.6	41
46	Impact of nitrogen vacancies on the high temperature behavior of (Ti1â^'xAlx)Ny alloys. Acta Materialia, 2016, 119, 218-228.	3.8	41
47	Fabrication of Well-Ordered High-Aspect-Ratio Nanopore Arrays in TiO2 Single Crystals. Nano Letters, 2006, 6, 1065-1068.	4.5	40
48	Stabilities of multiply charged dimers and clusters of fullerenes. Journal of Chemical Physics, 2007, 126, 224303.	1.2	39
49	Age hardening in (Ti 1â^'x Al x )B 2+Δ thin films. Scripta Materialia, 2017, 127, 122-126.	2.6	38
50	Effects of volume mismatch and electronic structure on the decomposition of ScAlN and TiAlN solid solutions. Physical Review B, 2010, 81, .	1.1	37
51	Phase transformations in face centered cubic (Al0.32Cr0.68)2O3 thin films. Surface and Coatings Technology, 2012, 206, 3216-3222.	2.2	37
52	Double-to-Single Target Ionization Ratio for Electron Capture in Fastp-He Collisions. Physical Review Letters, 2002, 89, 163201.	2.9	36
53	Even-odd effects in the ionization cross sections of[C60]2and[C60C70]dimers. Physical Review A, 2007, 75, .	1.0	36
54	lon mass spectrometry investigations of the discharge during reactive high power pulsed and direct current magnetron sputtering of carbon in Ar and Ar/N2. Journal of Applied Physics, 2012, 112, .	1.1	36

#	Article	IF	CITATIONS
55	Channeling effects observed in energy-loss spectra of nitrogen ions scattered off a Pt(110) surface. Physical Review A, 2001, 64, .	1.0	35
56	Barriers for asymmetric fission of multiply chargedC60fullerenes. Physical Review A, 2003, 67, .	1.0	35
57	Direct current magnetron sputtered ZrB2 thin films on 4H-SiC(0001) and Si(100). Thin Solid Films, 2014, 550, 285-290.	0.8	35
58	Well-ordered nanopore arrays in rutile TiO2single crystals by swift heavy ion-beam lithography. Nanotechnology, 2007, 18, 305303.	1.3	34
59	10B multi-grid proportional gas counters for large area thermal neutron detectors. Nuclear Instruments and Methods in Physics Research, Section A: Accelerators, Spectrometers, Detectors and Associated Equipment, 2013, 720, 116-121.	0.7	33
60	Experimental and theoretical investigation of Cr1-xScxN solid solutions for thermoelectrics. Journal of Applied Physics, 2016, 120, .	1.1	33
61	Microscopic observations of metallic inclusions generated along the path of MeV clusters in CaF2. Nuclear Instruments & Methods in Physics Research B, 1998, 146, 399-404.	0.6	32
62	Two-center interference in fast proton–H2-electron transfer and excitation processes. Physical Review A, 2005, 72, .	1.0	31
63	Effect of ion-implantation-induced defects and Mg dopants on the thermoelectric properties of ScN. Physical Review B, 2018, 98, .	1.1	31
64	Electronic stopping of swift partially stripped molecules and clusters. Physical Review A, 2000, 61, .	1.0	30
65	Microstructure evolution of Ti–Si–C–Ag nanocomposite coatings deposited by DC magnetron sputtering. Acta Materialia, 2010, 58, 6592-6599.	3.8	30
66	Structural and mechanical properties of corundum and cubic (Al Cr1â^')2+O3â^' coatings grown by reactive cathodic arc evaporation in as-deposited and annealed states. Acta Materialia, 2013, 61, 4811-4822.	3.8	29
67	Multi-Grid detector for neutron spectroscopy: results obtained on time-of-flight spectrometer CNCS. Journal of Instrumentation, 2017, 12, P04030-P04030.	0.5	29
68	Transparent and conducting TiO2:Nb films made by sputter deposition: Application to spectrally selective solar reflectors. Solar Energy Materials and Solar Cells, 2010, 94, 75-79.	3.0	28
69	Magic and hot giant fullerenes formed inside ion irradiated weakly bound C60 clusters. Journal of Chemical Physics, 2010, 133, 104301.	1.2	28
70	SiN <sub><i>x</i></sub> Coatings Deposited by Reactive High Power Impulse Magnetron Sputtering: Process Parameters Influencing the Nitrogen Content. ACS Applied Materials & Interfaces, 2016, 8, 20385-20395.	4.0	28
71	lonization ofC70andC60molecules by slow highly charged ions: A comparison. Physical Review A, 2004, 69, .	1.0	27
72	Self-organized anisotropic (Zr1â^'Si )N nanocomposites grown by reactive sputter deposition. Acta Materialia. 2015. 82. 179-189.	3.8	27

#	Article	IF	CITATIONS
73	Recoil-ion momentum distributions for transfer ionization in fast proton-He collisions. Physical Review A, 2005, 72, .	1.0	25
74	ERDA of Ni–Al2O3/SiO2 solar thermal selective absorbers. Solar Energy Materials and Solar Cells, 2008, 92, 1177-1182.	3.0	25
75	Heavy ion beam-based nano- and micro-structuring of TiO2 single crystals using self-assembled masks. Nuclear Instruments & Methods in Physics Research B, 2008, 266, 3113-3119.	0.6	25
76	Epitaxial growth and electrical-transport properties of Ti7Si2C5 thin films synthesized by reactive sputter-deposition. Scripta Materialia, 2011, 65, 811-814.	2.6	25
77	Ti–B–C nanocomposite coatings deposited by magnetron sputtering. Applied Surface Science, 2012, 258, 9907-9912.	3.1	25
78	Si incorporation in Ti1â^'xSixN films grown on TiN(001) and (001)-faceted TiN(111) columns. Surface and Coatings Technology, 2014, 257, 121-128.	2.2	25
79	Ion tracks in amorphous SiO2 irradiated with low and high energy heavy ions. Nuclear Instruments & Methods in Physics Research B, 2006, 245, 269-273.	0.6	24
80	Influence of the Chemical Composition on the Phase Constitution and the Elastic Properties of RFâ€ <b>s</b> puttered Hydroxyapatite Coatings. Plasma Processes and Polymers, 2008, 5, 168-174.	1.6	24
81	Influence of the target composition on reactively sputtered titanium oxide films. Vacuum, 2009, 83, 1295-1298.	1.6	24
82	Pattern-induced magnetic anisotropy in FePt thin films by ion irradiation. Physical Review B, 2011, 83, .	1.1	24
83	Room-temperature heteroepitaxy of single-phase Al1â^'xInxN films with full composition range on isostructural wurtzite templates. Thin Solid Films, 2012, 524, 113-120.	0.8	24
84	A novel high-power pulse PECVD method. Surface and Coatings Technology, 2012, 206, 4562-4566.	2.2	24
85	Gas phase chemical vapor deposition chemistry of triethylboron probed by boron–carbon thin film deposition and quantum chemical calculations. Journal of Materials Chemistry C, 2015, 3, 10898-10906.	2.7	24
86	V0.5Mo0.5Nx/MgO(001): Composition, nanostructure, and mechanical properties as a function of film growth temperature. Acta Materialia, 2017, 126, 194-201.	3.8	23
87	Low Temperature CVD of Thin, Amorphous Boron arbon Films for Neutron Detectors. Chemical Vapor Deposition, 2012, 18, 221-224.	1.4	22
88	Characterization of plasma chemistry and ion energy in cathodic arc plasma from Ti-Si cathodes of different compositions. Journal of Applied Physics, 2013, 113, 163304.	1.1	22
89	UV-black rutile TiO2: An antireflective photocatalytic nanostructure. Journal of Applied Physics, 2015, 117, 074903.	1.1	22
90	Tracks in YIG induced by MeV C60 ions. Nuclear Instruments & Methods in Physics Research B, 1998, 135, 295-301.	0.6	21

#	Article	IF	CITATIONS
91	Formation of surface nanostructures on rutile (TiO <sub>2</sub> ): comparative study of low-energy cluster ion and high-energy monoatomic ion impact. Journal Physics D: Applied Physics, 2009, 42, 205303.	1.3	20
92	Phase-stabilization and substrate effects on nucleation and growth of (Ti,V) <i>n</i> +1GeC <i>n</i> thin films. Journal of Applied Physics, 2011, 110, .	1.1	20
93	X-ray Photoelectron Spectroscopy Analyses of the Electronic Structure of Polycrystalline Ti1-xAlxN Thin Films with 0 â‰ <b>û</b> €‰x â‰ <b>û</b> €‰0.96. Surface Science Spectra, 2014, 21, 35-49.	0.3	20
94	Ab initio calculations and experimental study of piezoelectric Y In1â^'N thin films deposited using reactive magnetron sputter epitaxy. Acta Materialia, 2016, 105, 199-206.	3.8	20
95	A comparative study of direct current magnetron sputtering and high power impulse magnetron sputtering processes for CNx thin film growth with different inert gases. Diamond and Related Materials, 2016, 64, 13-26.	1.8	20
96	Ti–Si–C–N thin films grown by reactive arc evaporation from Ti <sub>3</sub> SiC <sub>2</sub> cathodes. Journal of Materials Research, 2011, 26, 874-881.	1.2	19
97	Stabilization of electrons onArq+ions after slow collisions withC60. Physical Review A, 2001, 63, .	1.0	18
98	Surface channeling of 1 and 10 keV nitrogen ions on a Pt(110)(1×2) surface. Nuclear Instruments & Methods in Physics Research B, 2002, 193, 568-575.	0.6	18
99	Growth and structural properties of Mg:C thin films prepared by magnetron sputtering. Thin Solid Films, 2010, 518, 4225-4230.	0.8	18
100	Two-domain formation during the epitaxial growth of GaN (0001) on <i>c</i> -plane Al2O3 (0001) by high power impulse magnetron sputtering. Journal of Applied Physics, 2011, 110, .	1.1	18
101	Influence of inert gases on the reactive high power pulsed magnetron sputtering process of carbon-nitride thin films. Journal of Vacuum Science and Technology A: Vacuum, Surfaces and Films, 2013, 31, .	0.9	18
102	Silicon oxynitride films deposited by reactive high power impulse magnetron sputtering using nitrous oxide as a single-source precursor. Journal of Vacuum Science and Technology A: Vacuum, Surfaces and Films, 2015, 33, .	0.9	18
103	Synthesis of hydrogenated diamondlike carbon thin films using neon–acetylene based high power impulse magnetron sputtering discharges. Journal of Vacuum Science and Technology A: Vacuum, Surfaces and Films, 2016, 34, 061504.	0.9	18
104	Continuous and Localized Mn Implantation of ZnO. Nanoscale Research Letters, 2009, 4, 878-887.	3.1	17
105	Effect of spatial defect distribution on the electrical behavior of prominent vacancy point defects in swift-ion implanted Si. Physical Review B, 2009, 79, .	1.1	17
106	Reactive high power impulse magnetron sputtering of CFx thin films in mixed Ar/CF4 and Ar/C4F8 discharges. Thin Solid Films, 2013, 542, 21-30.	0.8	17
107	Low-temperature growth of low friction wear-resistant amorphous carbon nitride thin films by mid-frequency, high power impulse, and direct current magnetron sputtering. Journal of Vacuum Science and Technology A: Vacuum, Surfaces and Films, 2015, 33, .	0.9	17
108	Electron capture and loss by protonated peptides and proteins in collisions with \$ mathsf {C_{60}}\$ and Na. European Physical Journal D, 2003, 22, 75-79.	0.6	16

#	Article	IF	CITATIONS
109	On the exciton model for ion-beam damage: The example of TiO2. Nuclear Instruments & Methods in Physics Research B, 2010, 268, 3122-3126.	0.6	16
110	Structure and morphology of nickel-alumina/silica solar thermal selective absorbers. Journal of Non-Crystalline Solids, 2011, 357, 1370-1375.	1.5	16
111	Step-flow growth of nanolaminate Ti3SiC2 epitaxial layers on 4H-SiC(0001). Scripta Materialia, 2011, 64, 1141-1144.	2.6	16
112	Reactive magnetron sputtering of uniform yttria-stabilized zirconia coatings in an industrial setup. Surface and Coatings Technology, 2012, 206, 4126-4131.	2.2	16
113	Influence of Ti–Si cathode grain size on the cathodic arc process and resulting Ti–Si–N coatings. Surface and Coatings Technology, 2013, 235, 637-647.	2.2	16
114	Principles for designing sputtering-based strategies for high-rate synthesis of dense and hard hydrogenated amorphous carbon thin films. Diamond and Related Materials, 2014, 44, 117-122.	1.8	16
115	Effects of low-fluence swift iodine ion bombardment on the crystallization of ion-beam-synthesized silicon carbide. Journal of Applied Physics, 2007, 101, 084311.	1.1	15
116	Arc deposition of Ti–Si–C–N thin films from binary and ternary cathodes — Comparing sources of C. Surface and Coatings Technology, 2012, 213, 145-154.	2.2	15
117	Epitaxial V0.6W0.4N/MgO(001): Evidence for ordering on the cation sublattice. Journal of Vacuum Science and Technology A: Vacuum, Surfaces and Films, 2013, 31, .	0.9	15
118	Silicon carbonitride thin films deposited by reactive high power impulse magnetron sputtering. Surface and Coatings Technology, 2018, 335, 248-256.	2.2	14
119	Electrostatic model calculations of fission barriers for fullerene ions. European Physical Journal D, 2004, 29, 63-68.	0.6	13
120	Experimental determination of electronic stopping for ions in silicon dioxide. Applied Physics Letters, 2005, 87, 104103.	1.5	13
121	Visualization of MeV ion impacts in Si using scanning capacitance microscopy. Physical Review B, 2006, 73, .	1.1	13
122	Surface patterning by heavy ion lithography using self-assembled colloidal masks. Nuclear Instruments & Methods in Physics Research B, 2007, 257, 777-781.	0.6	13
123	Patterning of rutile TiO <sub>2</sub> surface by ion beam lithography through full-solid masks. Nanotechnology, 2010, 21, 235301.	1.3	13
124	Energy-loss straggling of 2–10 MeV/u Kr ions in gases. European Physical Journal D, 2013, 67, 1.	0.6	13
125	Energy loss of fast N+ ions scattered off a Pt(1 1 0) surface. Nuclear Instruments & Methods in Physics Research B, 2000, 164-165, 566-574.	0.6	12
126	Crystalline quality of 3C-SiC formed by high-fluence C+-implanted Si. Applied Surface Science, 2007, 253, 4836-4842.	3.1	12

#	Article	IF	CITATIONS
127	On the effect of water and oxygen in chemical vapor deposition of boron nitride. Thin Solid Films, 2012, 520, 5889-5893.	0.8	12
128	Infrared dielectric functions and optical phonons of wurtzite Y <sub><i>x</i></sub> Al <sub>1â~<i>x</i></sub> N (0  ⩽  a€≪i>x   ⩽ â 48, 415102.	€‰ <b>0</b> 322).	Jou <b>t¤</b> al Physic
129	Electronic stopping forces of heavy ions in metal oxides. Nuclear Instruments & Methods in Physics Research B, 2006, 249, 18-21.	0.6	11
130	Electronic stopping powers for heavy ions in niobium and tantalum pentoxides. Nuclear Instruments & Methods in Physics Research B, 2006, 250, 62-65.	0.6	11
131	Growth and properties of amorphous Ti–B–Si–N thin films deposited by hybrid HIPIMS/DC-magnetron co-sputtering from TiB2 and Si targets. Surface and Coatings Technology, 2014, 259, 442-447.	2.2	11
132	Trimethylboron as Single-Source Precursor for Boron–Carbon Thin Film Synthesis by Plasma Chemical Vapor Deposition. Journal of Physical Chemistry C, 2016, 120, 21990-21997.	1.5	11
133	Dopant distribution in high fluence Fe implanted GaN. Journal of Applied Physics, 2008, 104, 053509.	1.1	10
134	Reduced photoluminescence from InGaN/GaN multiple quantum well structures following 40Mev iodine ion irradiation. Physica B: Condensed Matter, 2009, 404, 4925-4928.	1.3	10
135	Effects of A-elements (A Si, Ge or Sn) on the structure and electrical contact properties of Ti–A–C–Ag nanocomposites. Thin Solid Films, 2012, 520, 5128-5136.	0.8	10
136	β-Ta and α-Cr thin films deposited by high power impulse magnetron sputtering and direct current magnetron sputtering in hydrogen containing plasmas. Physica B: Condensed Matter, 2014, 439, 3-8.	1.3	10
137	Synthesis and characterization of Zr2Al3C4 thin films. Thin Solid Films, 2015, 595, 142-147.	0.8	10
138	Orientational dependence of electronic stopping of molecule and cluster ions. Nuclear Instruments & Methods in Physics Research B, 1994, 88, 191-195.	0.6	9
139	Nanopattern transfer to SiO[sub 2] by ion track lithography and highly selective HF vapor etching. Journal of Vacuum Science & Technology B, 2007, 25, 862.	1.3	9
140	Stopping power measurements of He ions in Si and SiC by time-of-flight spectrometry. Nuclear Instruments & Methods in Physics Research B, 2007, 261, 1180-1183.	0.6	9
141	FePt thin film irradiated with high energy ions. Physica Status Solidi (A) Applications and Materials Science, 2007, 204, 1724-1730.	0.8	9
142	Growth and characterization of epitaxial Ti3GeC2 thin films on 4H-SiC(0001). Journal of Crystal Growth, 2012, 343, 133-137.	0.7	9
143	Thermal stability and mechanical properties of amorphous coatings in the Ti-B-Si-Al-N system grown by cathodic arc evaporation from TiB2, Ti33Al67, and Ti85Si15 cathodes. Journal of Vacuum Science and Technology A: Vacuum, Surfaces and Films, 2014, 32, .	0.9	9
144	Compositional dependence of epitaxial Tin+1SiCn MAX-phase thin films grown from a Ti3SiC2 compound target. Journal of Vacuum Science and Technology A: Vacuum, Surfaces and Films, 2019, 37, .	0.9	8

#	Article	IF	CITATIONS
145	Carbon nanopillar array deposition on by ion irradiation through a porous alumina template. Vacuum, 2007, 82, 359-362.	1.6	7
146	Thermal instability of implanted Mn ions in ZnO. Journal of Applied Physics, 2010, 107, 023507.	1.1	7
147	Reactive sputtering of δ-ZrH2 thin films by high power impulse magnetron sputtering and direct current magnetron sputtering. Journal of Vacuum Science and Technology A: Vacuum, Surfaces and Films, 2014, 32, .	0.9	7
148	Investigation of background in large-area neutron detectors due to alpha emission from impurities in aluminium. Journal of Instrumentation, 2015, 10, P10019-P10019.	0.5	7
149	Novel hard, tough HfAlSiN multilayers, defined by alternating Si bond structure, deposited using modulated high-flux, low-energy ion irradiation of the growing film. Journal of Vacuum Science and Technology A: Vacuum, Surfaces and Films, 2015, 33, .	0.9	7
150	Energy releases in the fission of multiply charged C 60 ions. Nuclear Instruments & Methods in Physics Research B, 2003, 205, 643-650.	0.6	6
151	Transfer ionization in p+He collisions. Nuclear Instruments & Methods in Physics Research B, 2005, 233, 43-47.	0.6	6
152	Implantation of anatase thin film with 100 keV 56Fe ions: Damage formation and magnetic behaviour. Nuclear Instruments & Methods in Physics Research B, 2009, 267, 2725-2730.	0.6	6
153	Fragmentation of charged fullerene dimers: Kinetic energy release. Nuclear Instruments & Methods in Physics Research B, 2005, 235, 419-424.	0.6	5
154	Ion beams of carbon clusters and multiply charged fullerenes produced with electron cyclotron resonance ion sources. Review of Scientific Instruments, 2005, 76, 053304.	0.6	5
155	Fullerene collisions and clusters of fullerenes. International Journal of Mass Spectrometry, 2006, 252, 117-125.	0.7	5
156	Influence of pulse power amplitude on plasma properties and film deposition in high power pulsed plasma enhanced chemical vapor deposition. Journal of Vacuum Science and Technology A: Vacuum, Surfaces and Films, 2014, 32, 030602.	0.9	5
157	Selective binding of oligonucleotide on TiO 2 surfaces modified by swift heavy ion beam lithography. Nuclear Instruments & Methods in Physics Research B, 2014, 339, 67-74.	0.6	5
158	Formation of hydroxyapatite on titanium implants <i>in vivo</i> precedes bone-formation during healing. Biointerphases, 2017, 12, 041002.	0.6	5
159	Fragmentation and ionization of C70 and C60 by slow ions of intermediate charge. European Physical Journal D, 2006, 38, 299-306.	0.6	4
160	Activation energy of the growth of ion-beam-synthesized nano-crystalline 3C–SiC. Nuclear Instruments & Methods in Physics Research B, 2007, 257, 195-198.	0.6	4
161	Resolving mass spectral overlaps in atom probe tomography by isotopic substitutions – case of TiSi15N. Ultramicroscopy, 2018, 184, 51-60.	0.8	4
162	Effects on the structural and magnetic properties of amorphous ribbons of (Co0.94Fe0.06)72.5Si12.5B15 caused by 4MeV Cl2+ ion irradiation. Journal of Non-Crystalline Solids, 2007, 353, 879-882.	1.5	3

#	Article	IF	CITATIONS
163	Mapping of hydrogen isotopes with a scanning nuclear microprobe. Nuclear Instruments & Methods in Physics Research B, 2008, 266, 2429-2432.	0.6	3
164	High dose Fe implantation of GaN: damage build-up and dopant redistribution. Journal of Physics: Conference Series, 2008, 100, 042036.	0.3	3
165	Formation of basal plane fiberâ€textured Ti <sub>2</sub> AlN films on amorphous substrates. Physica Status Solidi - Rapid Research Letters, 2010, 4, 121-123.	1.2	3
166	Influence of Ar and N2Pressure on Plasma Chemistry, Ion Energy, and Thin Film Composition During Filtered Arc Deposition From Ti3SiC2Cathodes. IEEE Transactions on Plasma Science, 2014, 42, 3498-3507.	0.6	3
167	Influence of Si doping and O2 flow on arc-deposited (Al,Cr)2O3 coatings. Journal of Vacuum Science and Technology A: Vacuum, Surfaces and Films, 2019, 37, 061516.	0.9	3
168	Calculations of electronic energy loss of fast molecules in amorphous carbon. Nuclear Instruments & Methods in Physics Research B, 1996, 115, 39-42.	0.6	2
169	COLLISION INDUCED FRAGMENTATION OF FULLERENE CLUSTERS (C60)n. International Journal of Modern Physics B, 2005, 19, 2345-2352.	1.0	2
170	Multiple ionization and fragmentation of fullerene dimers by highly charged ion impact. Journal of Physics: Conference Series, 2007, 88, 012039.	0.3	2
171	Comparing XPS and ToF-ERDA measurement of high-k dielectric materials. Journal of Physics: Conference Series, 2008, 100, 012036.	0.3	2
172	Temperature effect on low-k dielectric thin films studied by ERDA. Journal of Physics: Conference Series, 2008, 100, 012041.	0.3	2
173	Stoichiometric silicon oxynitride thin films reactively sputtered in Ar/N2O plasmas by HiPIMS. Journal Physics D: Applied Physics, 2016, 49, 135309.	1.3	2
174	Azimuthal effects in grazing surface scattering. Journal of Electron Spectroscopy and Related Phenomena, 2003, 129, 309-313.	0.8	1
175	Transfer Ionization in MeV p-He Collisions Studied by Pulsed Recoil-Ion-Momentum Spectroscopy in a Storage Ring/Gas Target Experiment. AIP Conference Proceedings, 2003, , .	0.3	1
176	Localized56Fe+ion implantation of TiO2using anodic porous alumina. Materials Research Society Symposia Proceedings, 2009, 1181, 23.	0.1	1
177	Formation and annealing behavior of prominent point defects in MeV ion implanted n-type epitaxial Si. Materials Science and Engineering B: Solid-State Materials for Advanced Technology, 2009, 159-160, 177-181.	1.7	1
178	Localised modifications of anatase TiO2 thin films by a Focused Ion Beam. Nuclear Instruments & Methods in Physics Research B, 2010, 268, 3142-3146.	0.6	1
179	Structure and composition of Al(Si)CuFe approximant thin films formed by Si substrate diffusion. Thin Solid Films, 2014, 550, 105-109.	0.8	1

#	Article	IF	CITATIONS
181	Molecule and cluster bombardment: energy loss, trajectories, and collision cascades. , 1996, , 1-11.		1
182	Doppler Effect Derived from Time-Dependent Perturbation Theory. Journal of Molecular Spectroscopy, 1993, 158, 484-486.	0.4	0
183	Energy loss and charge state dependency of swift Nq+ ions scattered off a Pt()(1×2) surface. Nuclear Instruments & Methods in Physics Research B, 2003, 209, 259-264.	0.6	0
184	Scanning probe microscopy of single Au ion implants in Si. Materials Science and Engineering C, 2006, 26, 782-787.	3.8	0
185	Swift Heavy Ion Beam-Based Nanopatterning Using Self-Assembled Masks. Materials Research Society Symposia Proceedings, 2007, 1020, 1.	0.1	0
186	Measurement of hydrogen isotopes by a nuclear microprobe. Journal of Physics: Conference Series, 2008, 100, 062029.	0.3	0
187	Growth and oxidization stability of cubic Zr1â^'xGdxN solid solution thin films. Journal of Applied Physics, 2015, 117, 195301.	1.1	0
188	Energy loss and straggling of MeV Si ions in gases. Nuclear Instruments & Methods in Physics Research B, 2017, 391, 20-26.	0.6	0
189	STABILITY AND FRAGMENTATION OF HIGHLY CHARGED FULLERENE CLUSTERS. , 2004, , 301-311.		0
190	B-9 GIXRD CHARACTERIZATION OF ION BEAM SYNTHESIZED 3C-SiC(Session: Thin films). The Proceedings of the Asian Symposium on Materials and Processing, 2006, 2006, 32.	0.0	0
191	LIFETIMES OF \${m C}^{2-}_{60}\$ AND \${m C}^{2-}_{70}\$ DIANIONS IN A STORAGE RING. , 2006, , .		Ο